CAUSES, PRECURSORS AND MECHANISMS OF DISRUPTIONS IN ASDEX UPGRADE

G. Pautasso, P. Franzen, J.C. Fuchs, J. Gernhardt, O. Gruber, A. Kallenbach, K. Lackner, M. Maraschek, V. Mertens, H. Pfeiffer[1], W. Schneider, C. Tichmann, ASDEX Upgrade Team, NBI, ICRH and ECRH Groups

Max-Planck-Institut für Plasmaphysik, EURATOM Association
[1] *University of Bayreuth, Germany*

1. Introduction

A large number of disruptions in flat-top (520 plasmas with 173 disruptions in flat-top) were analyzed with the purpose of finding the technical causes, the precursors and the physical mechanisms of the disruptions. In the following we present the results of our analysis and suggestions to develop disruption recognition algorithms.

2. Technical and operational causes

The technical cause of the disruption is often identified after the shot and the presumed cause is recorded in the Journal by the session leaders. The information contained in the Journal was supplemented by our analysis and the causes of disruptions have been subdivided in the categories listed in Table 1. The results of this analysis are positive: 1) we found an initiating event for all the disruptions analyzed; in addition 2) we found that most of the disruptions could be attributed to some technical external cause and could be classified as *avoidable.*

Figures 1 summarizes the causes of disruptions and shows the percentage of shots which disrupted because of a given initiating event. The initiating events are indicated with a number and the description of the number is given in Table 1. The most frequent causes of a disruption were "planned density limit, with and without NI" followed by "NI turned off", "outer limiter" and "CDH (impurity seading) with q=3".

3. MHD precursors

The most familiar MHD scenario leading to a disruption is the one in which a rotating island exponentially grows within a few tenths of ms, it is slowed down by the electromagnetic interaction with the vessel, it locks and keeps growing until the final disruption. The Mirnov coils data can show a variety of scenarios, different from the above ideal case. The exponential growth, as seen by the Mirnov coils, can, for example, be replaced by a less defined, often sudden, growth of an island, rotating sometimes very slowly.

We compiled a list of locked mode durations for the range of shots analyzed. For this work we had to identify them by visual inspection of the Mirnov coils data. A locked mode detector for n=1, able to recognize a locked mode automatically, is now in operation and it is presently being optimized. In the cases where the locked mode phase was not clearly identified, *the duration* indicates the time between the development of some MHD activity, which seems to be responsible for the disruption, and the disruption itself. The locked mode phase was found to range from 430 ms (an exceptional long duration, since only two shots were found to have a locked mode phase longer than 250 ms) to a few ms.

Figure 2 shows that 1) a large number of discharges have a rather short (less than 30 ms, let's say) locked mode phase and that 2) the disruptions during NBI and at low q95 have a shorter locked mode phase than the disruption after NI or in ohmic plasmas and at large q95. We did not find any simple correlation between locked mode duration and disruption causes.

4. Mechanisms of disruptions

The better known chain of mechanisms leading to a disruption is triggered by the cooling of the plasma edge: the increased resistivity of the edge causes the peaking of the current profile (increase of the internal inductance, li) and the growth of the m=2/n=1 islands at the q=2 surface. The locking of this mode and its interaction with other modes lead then through a series of minor disruptions towards the final plasma quench. The cooling of the plasma edge can be achieved in different ways (because of high electron density, of high impurity density at the edge, contact with the wall) and in AUG it is typically accompanied by a MARFE in the X-point region. *As we are going to see, the majority of our disruptions can be interpreted according to this mechanism; but a part of them cannot.* The different stages of the chain of mechanisms of a *cold-edge disruption* can be clearly identified in a number of diagnostics: a MARFE which develops can be clearly seen by the bolometer and recognized by the MARFE-indicator signal "bli7/bli11" (bli7 and bli11 are two bolometer channels looking horizontally respectively below and above the X-point; see also Ref. [1]); li just before disruption (li_{disr}) are often well above the upper boundary of the steady state operational region [2] in the li-q diagram (li_{ss}).

With the simple condition: $$(li_{disr}/li_{ss} > 1) \quad .\text{and.} \quad (bli7/bli11 < 1) \qquad (1)$$

we could clearly separate the cold-edge disruptions from other disruptions, which have a different mechanism leading to them. In 74 % shots (1) indicates the cold-edge phase leading to disruption. In 15 % shots (1) indicates a MARFE before NI, which then disappears; (1) was also satisfied before disruption. In 11 % shots (1) is not satisfied. These last shots have mainly central impurity accumulation because of planned or not-planned impurity accumulation, during CDH shots with q=3, after beta-limit experiments and probably because of influx of gold from the ICRH antenna. Typically the shots with central impurity accumulation disrupt after the NBI are turned off; li remains low and the radiation from the plasma center is much higher than normal. Impurity accumulation in the plasma can also be easily detected with bolometer channels and automatically recognized due to the anomalously high central plasma radiation. The only shots in which the criteria (1) was not satisfied and no impurity accumulation is suspected were: one shot with VDE after loss of vertical control (detectable otherwise, monitoring the plasma position) and a few shots with density control above the Greenwald limit with pellets.

5. Neural network

Bolometer and li data were also used as input to a neural network which was trained by means of the back-propagation algorithm to detect the presence of a MARFE. The neural network used is a typical multilayer perceptron with one hidden layer consisting of 7 neurons. The neural network could detect reasonably well the presence of a MARFE and its output has the advantage of not relying on artificial and fixed stability thresholds (as condition (1)). An example of the neural network output is given in Fig. 3.

6. Conclusions

Disruptions in ASDEX Upgrade have well identified and, *at least in principle*, avoidable technical and operational causes. *Cold-edge* disruptions represent the majority of the disruptions and can easily be predicted by detecting locked mode and MARFE. These precursors detectors have already allowed successful avoidance (additional heating and closing of gas valves) and mitigation (gas puffing and killer pellets) experiments.

Work is in progress in order to make disruption prediction absolutely reliable and to determine the time of occurrence of a disruption.

References

[1] A. Kallenbach et al.: Plasma Physics and Controlled Fusion **38** (1996) 2097
[2] P. Franzen et al.: Fusion Technology **33** (1998) 1

code n.	cause description
1,2,3	Ne, C, SiC killer-pellet
5	only gas from killer-pellet injector
10	planned standard OH DL
11	not planned OH DL
12	excessive H/D puff
13	planned DL with NI
14	not planned DL with NI
20	NI turned off as planned
21	NI turned off (as planned ?)
22	NI turned off because of small density
23	NI turned off because of E-limit
24	NI turned off because of arcs in the NI sources
25	NI turned off because of cooling system
26	NI turned off, as planned, after beta limit exp.
30	control error
31	wrong ramp-up
32	saturated OH coils
33	outer limiter
34	disturbances of ICRH on the magnetic data
40	impurity event (not better identified)
41	excessive impurity puff
42	not planned impurity accumulation
43	planned W accumulation
44	W event
45	emitting probe
46	CDH mode with q=3

Table 1: List of the causes of disruption in ASDEX Upgrade
(the code number refers to Figure 1)

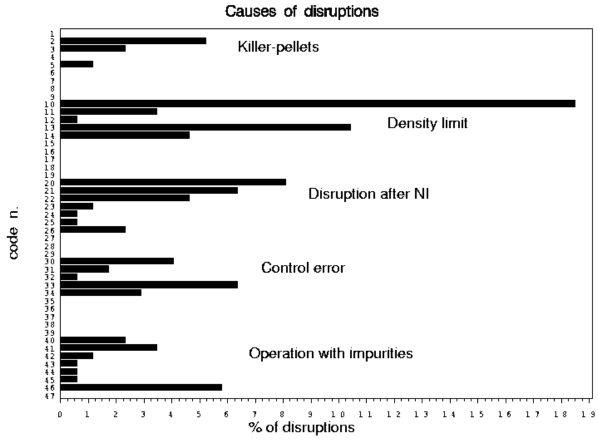

Fig. 1: The occurrence of disruptions according to their causes (code number refers to Table 1)

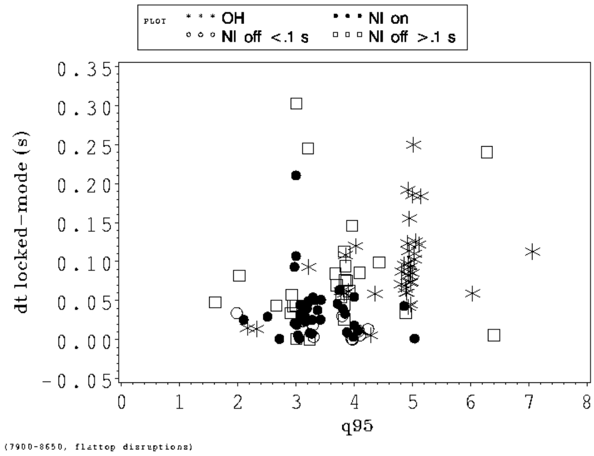

Fig. 2: Locked mode duration (dt) as function of q95

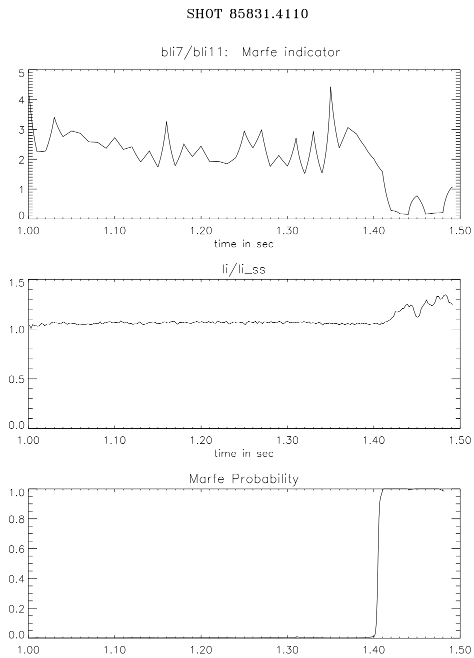

Fig. 3: Neural network prediction of a MARFE: the ratio between two bolometer signals, bli7/bli11, and the normalized plasma inductance, li_{disr}/li_{ss} were given as input to the network which was trained to predict the presence of a MARFE.